A Theoretical Study on the Kinetics of Disproportionation versus Association Reaction of $CH_3 + C_2H_5$

S. Hosein Mousavipour* and Zahra Homayoon

Department of Chemistry, College of Sciences, Shiraz University, Shiraz, Iran

Received: May 8, 2003; In Final Form: August 7, 2003

Two possible reaction paths for the $CH_3 + C_2H_5$ system are direct hydrogen abstraction or association reaction. In the present study, the kinetics of the two possible reactions are investigated from a theoretical point of view. Unimolecular dissociation of propane is also studied. As one expects, association or dissociation reactions are pressure dependent processes, while hydrogen abstraction reaction is not sensitive to the pressure. Potential energy surfaces for both reaction paths are explored by UMP2, CAS, QCISD, and DFT methods. Energies of stationary points were calculated by CASMP2, B3LYP, MP4SDTQ, and QCISD methods. Canonical variational transition-state theory and microcanonical variational RRKM calculations were used to locate the position of bottleneck for the association reaction of methyl and ethyl radicals. The RRKM method was used to calculate the pressure dependency of the rate constants for dissociation of propane and association of methyl and ethyl radicals. Conventional transition-state theory was used to calculate the rate constant for hydrogen abstraction reaction of the two radicals in the title in a temperature range of 200−2500 K. According to our RRKM calculations, the high-pressure Arrhenius parameters for dissociation reaction of propane and association reaction of the two radicals were found as $k_{-1} = 1.1 \times 10^{17}$ exp(−369.1 kJ mol^{-1}/RT) s^{-1} and $k_1 = 5.5 \times 10^{11}$ T$^{-0.56}$ exp(0.53 kJ mol^{-1}/RT) L mol^{-1}s^{-1}. According to generalized transition-state theory, the rate constant for hydrogen abstraction reaction were found as $k_2 = 9.8 \times 10^8$ L mol^{-1}s^{-1} over the temperature range of 200−2500 K.

Introduction

Gas phase radical−radical reactions have been extensively studied because of their importance in the chemistry of combustion, hydrocarbon cracking, air pollution, etc. As one expects, the rate constant for radical−radical association reactions are pressure dependent, while the rate constant of radical−radical disproportionation reactions are expected to be independent to the pressure. Most of the experimental studies on the radical−radical reactions have been monitored by means of end-product analysis in a complex system. If a particular product arises in more than one step in a complex system, it would be difficult to estimate the role of each step in the formation of that particular product.

One of the radical−radical reactions whose kinetics has been studied experimentally and reviewed to some extent is the $CH_3 + C_2H_5$ system. Two possible reaction paths have been suggested for this system.

$$CH_3 + C_2H_5 \rightarrow C_3H_8 \qquad \text{(R1)}$$

$$CH_3 + C_2H_5 \rightarrow CH_4 + C_2H_4 \qquad \text{(R2)}$$

Reaction R1 is an association reaction with a pressure dependent rate constant, while reaction R2 is a hydrogen abstraction reaction with no pressure dependent rate constant. Highly excited products are normally produced in the association reactions, and therefore it is necessary to remove the excess energy from the newly formed species by collisions to stabilize the product; however, this is not the case for disproportionation reactions. Normally, in disproportionation reactions, some part of the energy is consumed during the course of the reaction. Although these two reactions are studied by different groups, there are still some unanswered questions about the kinetics of this system. In most of the experimental and reviewed studies, reported values for the rate constant k_2 are much smaller than the reported values of k_1, and some researchers have just reported the ratio of k_2/k_1, which lies in a range of 0.035−0.060.[1]

In 1962, Thynne[2] studied hydrogen abstraction from ethyl radicals by methyl radicals in a temperature range of 351−521 K and reported the rate constant for this hydrogen abstraction reaction to have a temperature-independent value of $k_2 = 5.5 \times 10^9$ Lmol^{-1} s^{-1}.

Teng and Jones[3] in 1972 studied the kinetics of reaction of hydrogen atoms with ethylene and vinyl fluoride in a flow system in the temperature range of 303−603 K and in a pressure of 1.20 Torr. They reported the rate constant for the association reaction of methyl radicals with ethyl radicals as $k_1 = 2.51 \times 10^{10}$ exp (−1.67 kJ mol^{-1}/RT) L mol^{-1}s^{-1}. They did not report any data for reaction R2.

In 1975, Lifshitz and Frenklach[4] studied the mechanism of the thermal decomposition of propane behind reflected shocks. They accepted a value of 2.4×10^9 L mol^{-1}s^{-1} for the combination of these radicals in a temperature range around 1200 K and a pressure range of 50−200 Torr. In their work, it was not possible to measure k_1 directly in a system in which the decomposition of propane is being studied.

Koike and Gardiner[5] have studied the thermal decomposition of propane in reflected shock waves by IR laser absorption kinetic spectroscopy in a temperature range of 1300−1700 K near atmospheric pressure. In their study, they suggested 44 reactions that could incorporate in the pyrolysis of propane, and therefore analysis of such a system could not be very accurate

* To whom correspondence should be addressed. E-mail: mousavi@chem.susc.ac.ir.

10.1021/jp030597f CCC: $25.00
Published on Web 09/23/2003

TABLE 1: Reported Kinetic Parameters for Association and Hydrogen Abstraction Reactions of $CH_3 + C_2H_5$ in the Literature. A Factors in L $Mol^{-1}s^{-1}$ and Energies in KJ Mol^{-1}

k_1	k_2	T(K)	P(Torr)	ref
	5.50×10^9	351−521		2
3.37×10^{10}		300−2000	high p	12(b)
2.8×10^{10}	1.15×10^9	300−800	high p	12(a)
$1.9 \times 10^{11} \times T^{-0.32}$		773−2300	high p	46
2.7×10^{10}	9.9×10^8	308		7
$4.9 \times 10^{11} \times T^{-0.50}$	$1.95 \times 10^{10}\, T^{-0.5}$	300−2500	high p	11
7.0×10^9		300−2000	high p	9
$4.2 \times 10^{61} \times T^{-16.1} \exp(-1900/T)$		100−300	*a*	47
$8.9 \times 10^9 \exp(855/T)$		773.793	200	48
2.7×10^{10}		308		49
$8.0 \times 10^7 \exp(5700\ K/T)$	1×10^{10}	1300−1700	279	6
7.2×10^9	1×10^{10}	1300−1700	760	5
2.4×10^9		1050−1250	50−200	4
$2.5 \times 10^{10} \exp(-1.67/RT)$		303−603	1.20	3
4×10^{10}		290	8−16	50
4.2×10^{10}		373		51
$1.4 \times 10^{10} \exp(+3.6/RT)$		297−800	high p	13

[a] Termolecular reaction at low pressure.

without more information about the fall off behavior of some unimolecular reactions involved in the mechanism. In their suggested mechanism, ethylene was produced in nine different elementary reactions, and therefore the analysis of such a system to obtain any information about the kinetics of reaction R2 is rather difficult. They reported values of the rate constant for the combination reaction R1 as 7.2×10^9 L $mol^{-1}s^{-1}$ and for hydrogen abstraction reaction R2 as 1×10^{10} L $mol^{-1}s^{-1}$.

Simmie, Gardiner, and Eubank[6] in 1982 investigated the thermal dissociation of propane over the temperature range of 1300−1700 K and in a pressure of 279 Torr in a reflected shock wave experiment with the same mechanism suggested by Koike and Gardiner.[5] They reported the rate constant expression for the association reaction R1 as 8×10^7 exp (+5700 K/T) L $mol^{-1}s^{-1}$ and a temperature-independent value of 1×10^{10} L $mol^{-1}s^{-1}$ for the hydrogen abstraction reaction R2.

In 1987, Anastasi and Arthur[7] studied the combination and disproportionation reactions of CH_3 radicals with C_2H_5, *i*-C_3H_7, and *t*-C_4H_9 radicals. They monitored the concentration of radicals by means of molecular modulation spectroscopy. They reported values of $(9.9 \pm 0.7) \times 10^8$ L $mol^{-1}s^{-1}$ for hydrogen abstraction from ethyl radicals by methyl radicals and 2.7×10^{10} for combination of CH_3 and C_2H_5 at 308 K. No pressure range is reported in their results.

Garland and Bayes[8] in an investigation of the geometric mean rule for some radical−radical cross-reactions reported a value of $(9.3 \pm 4.2) \times 10^8$ L $mol^{-1}s^{-1}$ for the rate constant for reaction R1 at 300 K. In their study, they did not attempt to look at the possible hydrogen abstraction reactions.

In a review in 1984, Warnatz[9] suggested the rate constant for association reaction R1 as 7×10^9 L $mol^{-1}s^{-1}$ at 300−2500. In 1993, Sillesen and co-workers[10] reported a value of $4.0 \pm 0.2 \times 10^{10}$ L $mol^{-1}s^{-1}$ for the rate constant of overall reaction of CH_3+C_2H_5 at 298 K and a total pressure of 100 mbar.

These reactions were also reviewed by Tsang and Hampson[11] in 1986 in a temperature range of 300−2500 K. They obtained the rate constant for the association reaction of CH_3 and C_2H_5 as $k_1 = 4.89 \times 10^{11} \times T^{-0.5}$ L $mol^{-1}s^{-1}$ and for the disproportionation reaction of these two radicals as $k_2 = 1.95 \times 10^{10}\, T^{-0.5}$ L $mol^{-1}s^{-1}$.

In an extensive literature review in 1992, Baulch and co-workers[12] reported a value of $1.1 \pm 0.2 \times 10^9$ L $mol^{-1}s^{-1}$ for the hydrogen abstraction reaction R2 and a value of 2.83×10^{10} L $mol^{-1}s^{-1}$ for association reaction R1 in a temperature range of 300−800 K. In 1994, again Baulch and co-workers in a review reported a value of 3.37×10^{10} L $mol^{-1}s^{-1}$ for the rate constant of association reaction R1.

In 2001, Knyazev and Slagle[13] studied the kinetics of reaction of methyl radicals with C_2H_5, C_3H_7, and C_4H_9 radicals. They reported their results for reaction R1 as $k_1^\infty = 1.4 \times 10^{10} \exp(+3.6\ kJ\ mol^{-1}/RT)$ L $mol^{-1}s^{-1}$.

The reported kinetic parameters for association and disproportionation reactions of ethyl radicals with methyl radicals in the literature are summarized in Table 1.

The rate constant for reaction R1 is pressure dependent. Warnatz[14] has calculated the effect of temperature on the fall off curves of some dissociation reactions. Dean[15] has studied the effect of temperature and pressure upon some recombination reactions. He used quantum RRK theory to predict the effect of pressure on the rate constant of association reactions. Becker[16] and co-workers have studied the temperature and pressure dependence of the reaction $CH + H_2 \rightarrow CH_3$. They used a model based on the RRKM theory to describe the behavior of fall off curve for CH_3 formation. Zhu, Chen, Hase, and Kaiser[17] have studied the effect of pressure and temperature on the rate of association reaction $Cl + C_2H_2$. In their study, they compared different models in RRKM theory to study the behavior of the association reaction of $Cl + C_2H_2$. Olzmann[18] has studied the role of bimolecular reactions in chemical activation systems. He calculated the branching ratio between unimolecular decomposition channel and the collisional stabilization under steady-state conditions.

In the present study, we used an RRKM-TST model to calculate the pressure and temperature dependency of reaction R1.

In summary, one could conclude from the literature review on the kinetics of reaction of $CH_3 + C_2H_5$ that although this reaction is studied by different groups there are still some questions about the ratio of rate constants k_1 and k_2 at high-pressure limit. From the literature review, see Table 1, it could be seen that most of the reported values of k_2 are smaller than the values reported for k_1. No barrier for reaction R2 is reported in the literature. Although the reaction path degeneracy for reaction R2 should be greater than that for reaction R1, 6/4, why should the rate constant for reaction R2 be smaller than the high-pressure rate constant for reaction R1? The aim of the present investigation was to perform a theoretical study on the potential energy surfaces of the two pathways R1 and R2 by using high level ab initio quantum chemical calculations and

to calculate their rate constants and try to find an answer for the above question.

The reverse of reaction R1 is unimolecular dissociation of propane.

$$C_3H_8 \rightarrow CH_3 + C_2H_5 \qquad \text{(R-1)}$$

The rate constant of reaction R−1 is pressure dependent. In the present study, we also investigated the effect of pressure and temperature on the rate constant for reaction R−1 according to RRKM theory.

Methods of Calculation. *Potential Energy Surfaces.* Ab initio calculations were carried out using the Gaussian98W program system.[19] All the geometries of the stationary points were optimized at the MP2/6-311+G(2d,2p) level of theory. The potential energy surfaces of reactions R1 and R2 were explored at the UMP2/6-311+G(2d,2p) level with mixed HOMO and LUMO option to destroy $\alpha-\beta$ and spatial symmetries. To locate the possible saddle point for reaction R2, we used the QST2 method utilized in the Gaussian98W program at the UMP2 and CAS level of theory.

To obtain more accurate energies along the potential energy surfaces, single point MP4SDTQ,[20] forth-order Moller−Plesset perturbation theory, CASMP2[21] calculations were carried out at the MP2 geometries. Stationary points were also re-optimized using the DFT method with Becke's three-parameter hybrid functional UB3LYP.[22] In MCSCF calculations, two electrons and two orbitals were specified in the active space for reaction R1 and four electrons, and four orbitals were specified in the active space for reaction R2.

The effect of the dynamic valence-electron correlation on the relative energies of calculated stationary points was incorporated by performing single-point calculations of QCISD = full method[23] on the MP2 geometries. Also more flexible 6-311++G-(3DF,2P) and 6-311++G(3DF,3PD) basis sets were used in our calculations.

The zero-point energies were determined from the MP2 and CAS harmonic vibrational term values. Calculated vibrational frequencies were scaled by a factor of 0.94.[24]

Heats of formation of CH_3, C_2H_5, C_2H_4, CH_4,[25] and C_3H_8[26] at 298 K were reported as 146.3 ± 0.5, 107 ± 6, 52.4, −74.6 ± 0.3, and −104.7 kJ mol^{-1}, respectively. According to these data, $\Delta H°$ for reactions R1 and R2 was found to equal −358.0 ± 6.5 kJ mol^{-1} and −275.5 ± 7.5 kJ mol^{-1} at 298 K, respectively. According to our calculations, $\Delta H°_{298}$ for reaction R1 was found to be −375.3 kJ mol^{-1} and −340.2 kJ mol^{-1} at the MP2/6-311++G(d,p) and B3LYP/6-311++G(2d,2p) levels, respectively, and for reaction R2, it was found to be −282.4 kJ mol^{-1} and −273.8 kJ mol^{-1} at the MP2/6-311++G(d,p) and B3LYP/6-311++G(2d,2p) levels, respectively. These results show a better agreement between the experimental values and the results from B3LYP calculations for $\Delta H°_{298}$.

Calculation of Rate Constants k_1 and k_2. There is no saddle point in association reactions such as reaction R1. Therefore, it is difficult to locate the position of the bottleneck for such reactions. To find the location of the transition state along the reaction coordinate, it was assumed that passage through a bottleneck at a particular distance limits the rate of the reaction.[27] Canonical variational transition state theory and microcanonical variational RRKM calculations were used to find the location of bottleneck for reaction R1. It can be shown that at the high-pressure and temperature limit, the expression for the rate constant derived from simple collision theory approaches the expression given for transition state theory.[28]

We started with the familiar, simple collision theory rate constant to find the location of bottleneck for reaction R1.[29]

$$k(T,R) = P(R)\pi R^2 u_r \exp[-V(R)/k_B T] \qquad (1)$$

Here $P(R)$ is the product of the quotient of electronic partition functions B_e (which in our calculations was set to equal 1/4) and rotational partition functions B_θ ($P(R)=B_eB_\theta$). B_θ is the quotient of partition functions for hindered and free rotations of the reactants with respect to tumbling or rocking angles, θ. To eliminate the effect of the low vibrational frequencies on the curvature of Arrhenius plot at high temperatures, we did not include low vibrational frequencies in the B_θ ratio. u_r is the relative velocity, R is the distance of the two reactants as the reaction proceeds, and $V(R)$ is the potential energy along the reaction coordinate. The degrees of freedom in the reactant can be divided into conserved modes and transitional modes.[30] Most of the vibrational modes do not change significantly from the reactants to the transition state and only some of them change as the reaction proceeds.

Because reactants in reaction R1 are nonlinear, their six external rotational degrees of freedom would be transformed to internal rotations or torsional modes and tumbling or rocking motions. The free rotational partition function for a nonlinear species will be

$$Q_{f,n} = 2^{4.5}\pi^{3.5}(k_B T)^{1.5}(I_x I_y I_z)^{0.5}/(h^3\sigma_n) \qquad (2)$$

If we assume the motion around the x axis, which joins the two reactants, can be treated as a free internal rotation, therefore the partition function for this motion can be written as

$$Q_{x,n} = (2\pi)^{1.5}(I_x k_B T)^{0.5}/h\sigma_x \qquad (3)$$

The other two rotations can be transformed to rocking or tumbling motions as two reactants approach each other. The classical partition function for these rocking or tumbling motions around the z and y axes have the following form for each reactant, which may not be degenerate:[31]

$$Q_{yz,n} = (k_B T/h\nu_y)(k_B T/h\nu_z) \qquad (4)$$

The force constant for each of these motions might be calculated as $F = I(2\pi\nu)^2$, where I is the moment of inertia. Combining eqs 2 and 4 yields the following expression for B_θ in eq 1:

$$B_\theta = \frac{\sigma k_B T}{(F_y F_z)^{1/2}} \qquad (5)$$

Here F_y and F_z are the force constants for those tumbling or rocking motions.

In the present study, we also performed microcanonical variational RRKM calculations[32] to locate the position of the transition state for association reaction R1 at different temperatures. A general RRKM program[33] was used to carry out this kind of calculation. To locate the position of the bottleneck for reaction R1, the unimolecular dissociation reaction of propane was studied. In RRKM calculations, the UB3LYP potential energy surface was used to calculate the sum of the states of the system at different C- - -C bond lengths for decomposition of propane. In this kind of calculation, the RRKM program searches the minimum in the sum of states versus reaction coordinate as a function of available energy to locate the position of the bottleneck.

Generalized transition state theory, eq 6, was used to calculate the rate constant for hydrogen abstraction reaction R2.[34]

$$k(T,s) = \Gamma \frac{k_B T}{h} \sigma \frac{Q^{\neq}(T,s)}{Q_A Q_B(T)} \exp\left(\frac{-V_{MEP}(s)}{k_B T}\right) \quad (6)$$

Here, Γ is the tunneling factor,[35] k_B and h are Boltzmann's and Planck's constants, resectively, T is the temperature, σ is the reaction path degeneracy (the ratio of symmetry numbers from the rotational partition functions), The Qs represent the products of rotational, vibrational, and translational partition functions for the transition state (numerator) and reactants (denominator), s is the distance along the reaction path, and V_{MEP} is the potential energy corrected for zero-point energy at the generalized transition state location s at zero degrees.

RRKM calculations was performed to find the rate constant expression for reactions R−1 and R1. For RRKM calculations a general RRKM program by Hase and Bunker was used[39] and modified to calculate the fall off region and high-pressure rate constant $k(T)$. The following expression is used to calculate the unimolecular rate constant for reaction R−1 as a function of pressure:[36]

$$k_{uni} = \sigma \frac{\beta_c Z[M]}{hQ_r} \exp\left(\frac{-E_0}{RT}\right) \Delta E^+ \sum \left[\frac{\{W(E^+_{vr})\} \exp\left(\frac{-E^+}{RT}\right)}{\beta_c Z[M] + k_a(E^*)} \right] \quad (7)$$

Here, σ is the statistical factor, Q_r represents the partition function for the reactant fragments at infinite separation, E_0 is the zero-point energy, E^+ is the total nonfixed energy of a given transition state, ΔE^+ is the energy increment, $W(E^+_{vr})$ is the sum of vibrational−rotational states of the transition state, $k_a(E^*)$ is the rate constant for conversion of energized molecule to products, β_c is the collisional deactivation efficiency, Z is the collision number, and $[M]$ is the concentration. The rate constant at infinite pressure is calculated according to the following equation:[37]

$$k_\infty = \frac{\sigma B_e}{hQ_r} \exp\left(\frac{-E_0}{RT}\right) \int_{E^+=0}^{\infty} \{W(E_{vr}{}^+)\} \exp\left(\frac{-E^+}{RT}\right) dE^+ \quad (8)$$

To calculate the effect of pressure and temperature on the rate constant for reaction R1, the following mechanism for association reaction of $CH_3 + C_2H_5$ can be written:

$$CH_3 + C_2H_5 \underset{k_{-1}}{\overset{k_1}{\rightleftharpoons}} C_3H_8^*$$

$$C_3H_8^* \xrightarrow{W} C_3H_8$$

Using this mechanism, the bimolecular association rate constant can be written as

$$k_{bi} = \frac{\sigma B_e}{hQ_r} \int dE^+ \sum_{J=0}^{\infty} \left[\frac{(2J+1)\{W(E^+_{vr})\} \exp\left(\frac{-E^+}{RT}\right)}{1 + \frac{k_{-1}}{\omega}} \right] \quad (9)$$

Where $\omega = \beta_c Z[A]$ and B_e in the ratio of electronic partition functions, which is equal to 1/4 for reaction R1. The rate constants were calculated in a temperature range of 200−2500 K. k_{-1} can be calculated as the ratio of the sum of states of the transition state over density of states of the reactant divided by Planck's constant ($k_{-1} = W(E^+)/h\,N(E^+)$). The sum and densities of states are determined by semiclassical counting procedure.[38] To find these parameters, the standard RRKM program for the reverse reaction of R1 was used.[39] The resulting expression for the high-pressure association rate constant is[39]

$$k_{bi} = \frac{\sigma B_e}{hQ_r} \int \sum_{J=0}^{\infty} (2J+1)\{W(E^+_{vr})\} \exp\left(\frac{-E^+}{RT}\right) dE^+ \quad (10)$$

The Laplace transformation of the integral part of eq 10 is partition function $Q^{\#}$ for the transition state multiplied by $k_B T$.[45] Therefore, eq 10 is equal to the expression given for the transition state theory, eq 6.

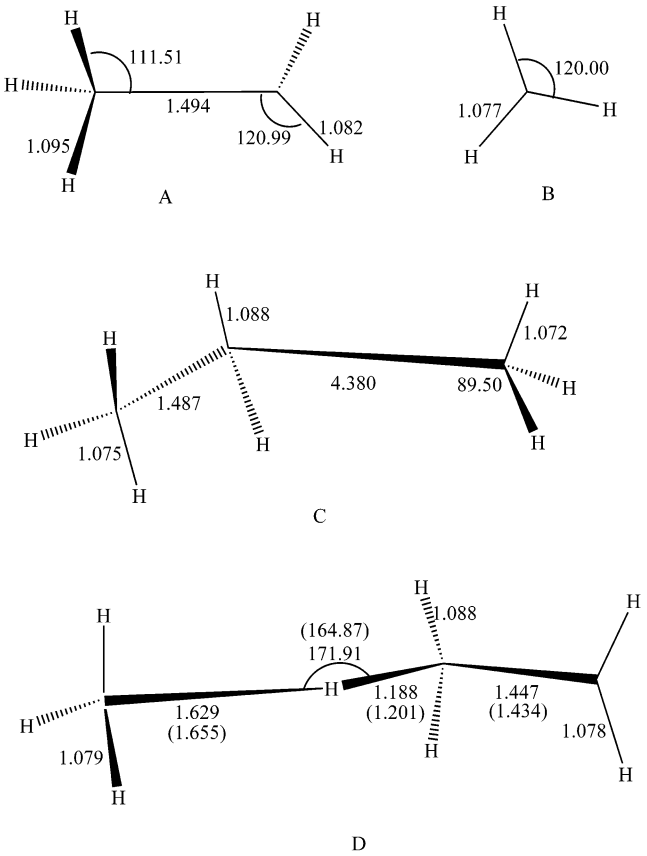

Figure 1. Optimized structures of ethyl(A), methyl (B), transition state of R1 (C), and transition state of R2 (D) at the MP2/6-311+G(2d,2p) level. Numbers in parentheses are from CAS(4,4)/6-31+G(d,p) results.

Results and Discussion

Reactions R1 and R−1. The geometries of reactants and transition state for reaction R1 along the minimum energy path were obtained at the MP2/6-311+G(2d,2p) level and shown in Figure 1. Ab initio molecular orbital calculations have been employed to determine the shape of the potential energy surface. Figure 2 shows schematic of potential energy surface for reaction R1 at the ump2/6-311+G(2d,2P), UB3LYP/6-311+G(2d,2P), CAS(2,2)/6-311+G(2d,2P), and QCISD = full/6-311+G(d,P) levels. To fit all the potential energy surfaces for reaction R1 in Figure 2, the results of CAS calculations are arbitrarily shifted by −0.5 hartree.

Total energies of reactants, activated complex, and product of reaction R1 at different levels of theory are listed in Table 2. Experimental bond strength D_0 for C—C bond in propane has been reported equal to 367.8 kJ mol^{-1} at 0 K.[40] The barrier heights corrected for zero-point energies for C—C dissociation

TABLE 2: Calculated Total Energies of All Species at Different Levels of Theory in amu

method of calc	CH_3	C_2H_5	[a]CH_3—C_2H_5	R2TS	C_3H_8	CH_4	C_2H_4
(P)MP2 = full 6-311+G(2d,2p)	−39.74217	−78.96858	−118.71075	−118.69999	−118.86197	−40.41412	−78.40796
MP4SDTQ = full 6-311+G(2d,2p)	−39.76492	−79.01005	−118.77497	−118.76924	−118.92558	−40.44086	−78.44790
CASMP2 6-311++G(d,p)	−39.73015	−78.94040	−118.67055	−118.66803	−118.80924	−40.38903	−78.08520
CASMP2 6-311+G(2d,2p)	−39.74286	−78.96468	−118.70784	−118.70652	−118.85471	−40.40747	−78.45950
CASMP2 6-311++G(3df,2p)	−39.75468	−78.99101	−118.74569	−118.74163	−118.89758	−40.42282	78.09128
B3LYP 6-311+G(2d,2p)	−39.85749	−79.18891	−119.04640	−119.04702	−119.18717	−40.53669	−78.61941
B3LYP 6-311++G(3df,3pd)	−39.85831	−79.19095	−119.04926	−119.05000	−119.19009	−40.53739	−78.62190
QCISD = full 6-311+G(2d,2p)	−39.76215	−79.00132	−118.76347	−118.75880	−118.90807	−40.43605	−78.43553

[a] Sum of total energies of CH_3 plus C_2H_5 at an infinite distance.

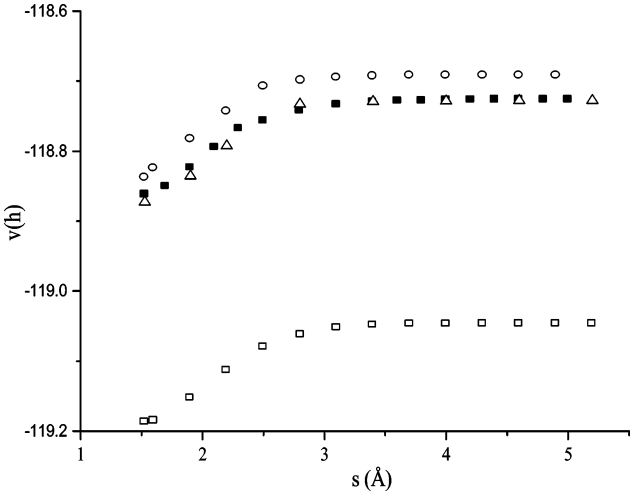

Figure 2. Potential energy surfaces for association reaction R1 at different levels of theory. (△) QCISD = full/6-311+G(d,p), (■) UMP2/6-311+G(d,p), (□) B3LYP/6-311+G(2d,2p), and (○) CAS(2,2)/6-311+(2d,2p).

TABLE 3: Barrier Heights Corrected for Zero-Point Energies for Dissociation Reaction of Propane (R−1) and Reaction R2 in kJ mol^{-1}

method of calc	R-1	R2
(P)MP2 = full/6-311+G(2d,2p)	386.4	26.1
MP4SDTQ = full/6-311+G(2d,2p)	384.8	12.9
CASMP2/6-311++G(d,p)	353.5	4.5
CASMP2/6-311+G(2d,2p)	375.7	1.4
CASMP2/6-311++G(3df,2p)	388.1	8.5
B3LYP/6-311+G(2d,2p)	358.9	0.5
B3LYP/6-311++G(3df,3pd)	359.1	0.2
QCISD = full/6-311+G(2d,2p)	369.0	10.1

in propane at different levels of theory is listed in Table 3. Vibrational frequencies and zero-point energies have shown in Table 4. Experimental vibrational term values for CH_3 and C_2H_5 were obtained from ref 41, and those for CH_4, C_2H_4, and C_3H_8 were obtained from ref 42. Moments of inertia for the reactants and the transition state are given in Table 5.

According to eq 1, the rate constant for reaction R1 has been calculated at different temperatures from 300 to 3000 K and for values of R_{C---C} between 2.5 and 8 Å. The results from UB3LYP method was used to calculate the rate constant for reaction R1 as a function of C- - -C distance and temperature. As shown in Table 3, activation energy for reaction R−1 (dissociation reaction of propane) is in good agreement with the experimental data reported in the NIST Chemical Kinetics Data Base[43] and in low cost of computation. The results are shown in Figure 3. As shown in Figure 3, on the UB3LYP surface, the bottleneck for the rate of reaction R1 was found at a C—C bond distance of 5 Å at lower temperatures. This value decreases to a value of 3.8 Å as temperature approaches 3000 K.

TABLE 4: Vibrational Term Values in cm^{-1} and Zero-Point Energies in amu of Reactants, Activated Complexes for Reactions R1 and R2[a]

CH_3	C_2H_5	R1 T. S.	R2 T. S.	C_3H_8	CH_4	C_2H_4
3161	3112	3184	3197	2977	3019(3)	3106
3161	3033	3184	3195	2973	2917	3103
3004	2987	3120	3117	2968	1534(2)	3026
1396	2987	3037	3094	2968	1306(3)	2989
1396	2842	3018	3093	2967		1623
606	1440	2957	3018	2962		1444
	1440	2939	2917	2887		1342
	1440	2905	1552	2887		1236
	1366	1530	1470	1476		1023
	1175	1519	1424	1472		949
	1175	1516	1422	1464		943
	1138	1473	1403	1462		826
	528	1450	1398	1451		
	528	1450	1191	1392		
	528	1222	1157	1378		
		1174	1047	1338		
		1043	989	1278		
		840	797	1192		
		631	628	1158		
		292	585	1054		
		262	566	940		
		262	465	922		
		235	378	869		
		192	173	748		
		192	155	369		
		165	116	268		
		35i	1245i	216		
ZPE 0.03064	0.06199	0.09650	0.09343	0.10042		

[a] Frequencies calculated at CAS/6-311G(d,p) level and scaled by 0.94. Frequencies of CH_3, C_2H_5, are from ref 41 and vibrational term values of C_2H_4, CH_4, and C_3H_8 Are from ref 42.

TABLE 5: Rotational Constants for Reactants and Activated Complexes of Reactions R1 and R2 and Propane in GHz

	B_1	B_2	B_3
CH_3	288.157	288.157	144.078
C_2H_5	103.685	22.632	20.970
R1TS	22.491	2.137	2.031
R2TS	28.435	4.185	3.929
C_3H_8	29.524	8.460	7.487

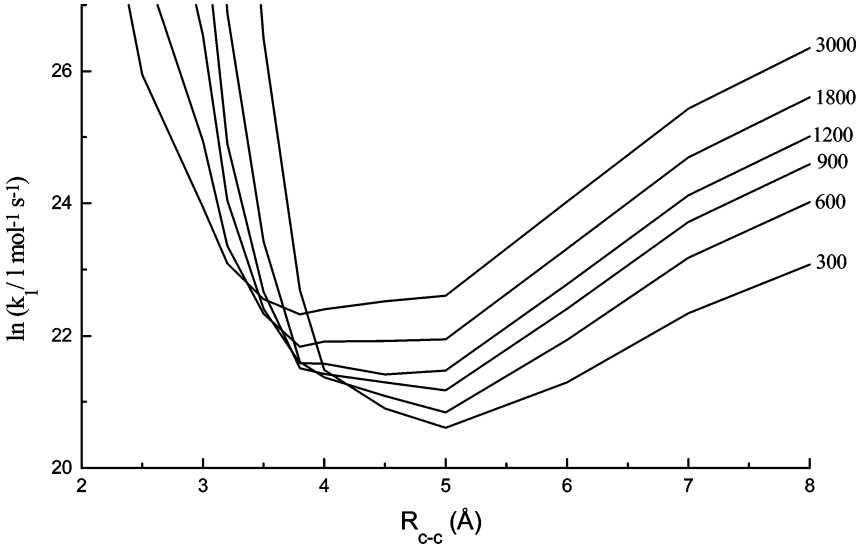

Figure 3. Calculated rate constant for association reaction of $CH_3 + C_2H_5$ as a function of C- - -C distance at different temperatures, eq 1.

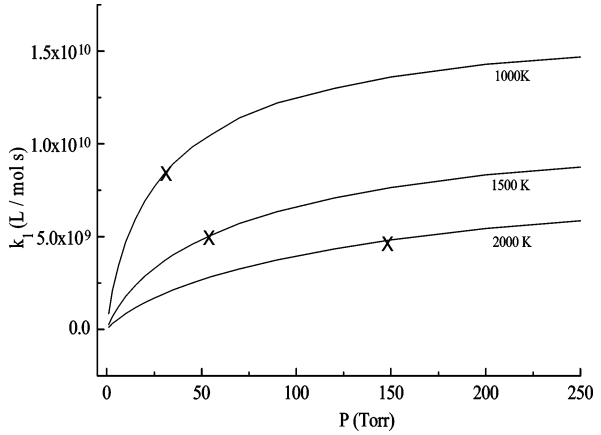

Figure 4. Fall off behavior of k_1 at three different temperatures. The Xs represent the position of $P_{1/2}$ at each temperature.

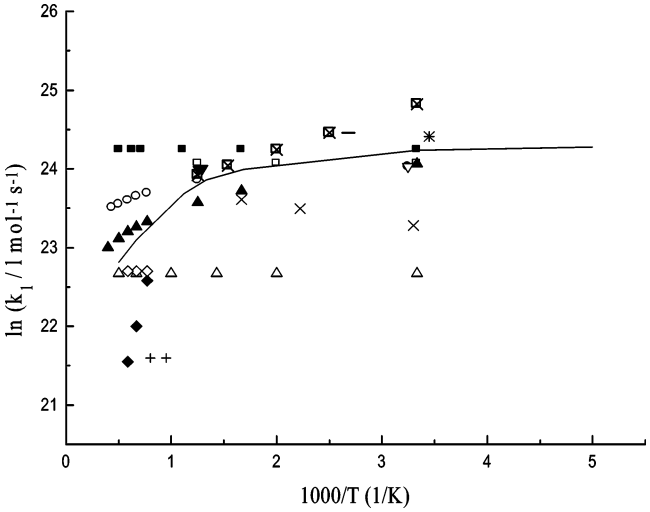

Figure 5. Arrhenius plot for association reaction R1. Solid line from eq 9. The symbols represent data from the following references, (−) ref 1e, (□) ref 12, (○) ref 19, (▽) ref 22, (X) ref 3, (△) ref 9, (◇) ref 5, (◆) ref 6, (■) ref 12b, (▼) ref 16, (▲) ref 11, (●) ref 7, (+) ref 4, (*) ref 18, and (boxed X) ref 13.

According to RRKM calculations, the position of the bottleneck for reaction R−1 was found to be 4.90 Å of C- - -C bond at lower temperatures (lower energies) and decreased to a value of 3.97 Å at higher energies. To search the bottleneck for reaction R−1 along the reaction coordinate, the moments of inertia and frequencies at each C- - -C bond length along the reaction coordinate were calculated. It was found that only two low vibrational term values and two moments of inertia were changing with changing the C- - -C bond length. Therefore, to find the bottleneck for reaction R−1 according to RRKM calculations, two low vibrational frequencies and two moments of inertia varied at each point along the reaction coordinate. In this kind of calculation, the RRKM program[39] gave the minimum rate constant $k(E)$ in a position along the reaction coordinate that the sum of states is minimum.

Fall off behavior of k_1 at three different temperatures is shown in Figure 4. According to RRKM theory, the solid curve in Figure 5 shows the Arrhenius plot for reaction R1 that is compared with the data from the literature. According to the solid line in Figure 5, the expression for k_1 was found as

$$k_1 = 5.5 \times 10^{11}\ T^{-0.56} \exp(0.53\ \text{kJ mol}^{-1}/RT)\ \text{L mol}^{-1}\text{s}^{-1}$$

The rate constant for dissociation of propane R−1 was calculated according to RRKM theory. To calculate the rate constant for reaction R−1, a value of 359.1 kJ mol^{-1} from DFT calculations was used for E_0. Figure 6 shows the falloff behavior of k_{-1} at 600 K. The Arrhenius plot for reaction R−1 is shown in Figure 7 and compared with selected data in the literature.[44] The Arrhenius parameters for reaction R−1 were found as

$$k_{-1} = 1.1 \times 10^{17} \exp(-369.1\ \text{kJ mol}^{-1}/\text{RT})\ \text{s}^{-1}$$

Reaction R2. Total energies of reactants, activated complex, and products of reaction R2 at the (P)MP2, MP4SDTQ, CASMP2, B3LYP, and QCISD = full levels are listed in Table 2. The potential energy surface along the minimum energy path for reaction R2 is shown in Figure 8. The search for the transition structure for reaction R2 was done by using the QST2 method utilized in the Gaussian98W. CAS(4,4)MP2, and UMP2 methods was used to locate the saddle point for reaction R2, which gave almost the same structure for the transition state. The geometry of the saddle point according to MP2 and CASMP2 calculations is shown in Figure 1, which is very similar to the structure of reactants at an infinite distance. The moments of inertia for the transition state are listed in Table 5. Figure 8 shows the intrinsic reaction coordinate (IRC) for reaction R2 at the ump2/6-311+G(2d,2p) level of theory.

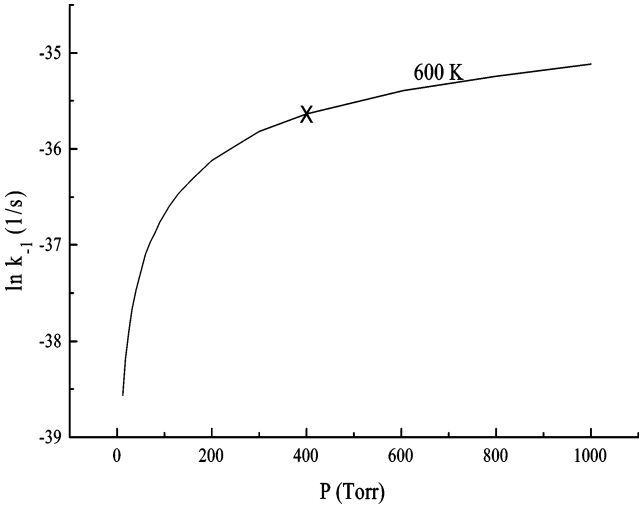

Figure 6. Fall off behavior of k_{-1} at 600 K. X represents the position of $P_{1/2}$.

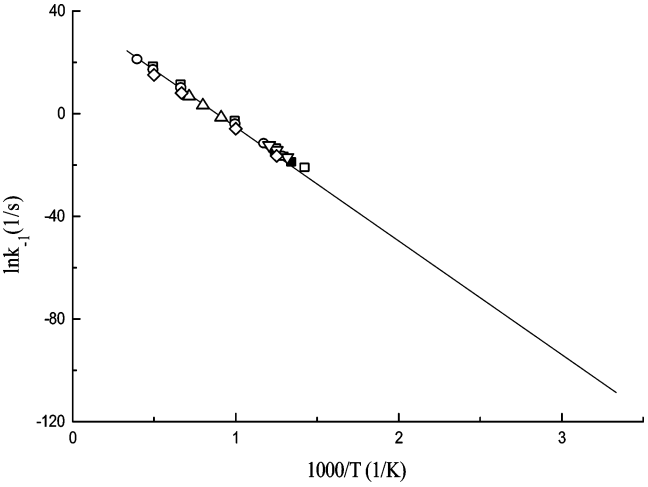

Figure 7. Arrhenius plot for reaction R−1. Solid line from RRKM theory. The symbols represent data from the following references, (■) ref 50a, (□) ref 12b, (○) ref 50b, (△) ref 50c, (▽) ref 50d, (◇) ref 50e.

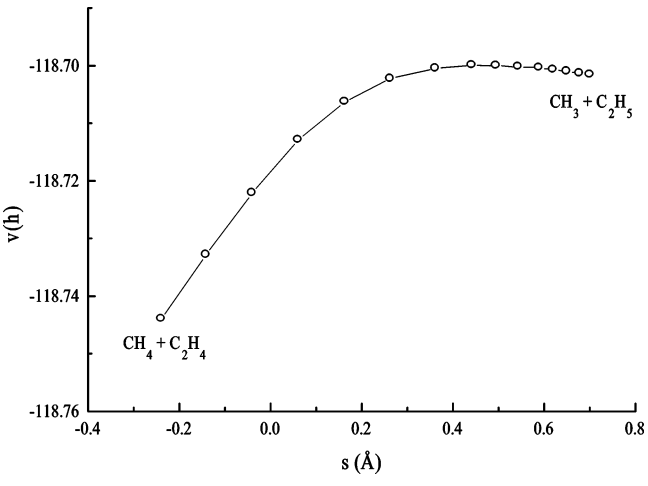

Figure 8. Potential energy surfaces for association reaction R2 at the UMP2/6-311+G(2d,2p) level of theory.

The reported barrier heights in Table 3 are corrected for the zero-point energies. As shown in Table 3, the barrier heights for reaction R2 calculated by (P)MP2, MP4SDTQ, and QCISD-(T) methods were almost the same, while MCSCF and DFT methods gave a lower barrier height for reaction R2.

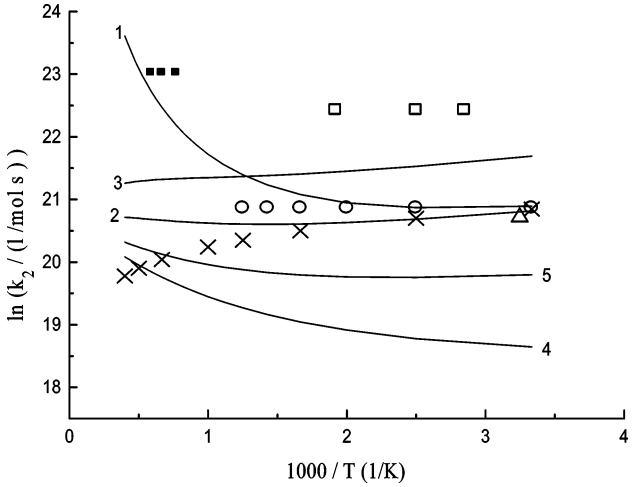

Figure 9. Arrhenius plot for disproportionation reaction R2. Curve 1 from DFT results with $E_0 = 0.5$ kJ mol^{-1} calculated by means of transition state theory, eq 6. Curve 2 is the same as curve 1 with no low vibrational term values included. Curve 3 is the same as curve 2 except $E_0 = 0.2$ kJ mol^{-1} from DFT results. Curve 4 is the same as curve 2 except no tunneling factor is included. Curve 5 is the same as curve 2 except $E_0 = 1.4$ kJ mol^{-1} from CASMP2 results. The symbols represent data from the following references, (○) ref 12a, (△) ref 7, (□) ref 2, (X) ref 11, and (■) ref's 5 and 6.

To calculate the rate constant for reaction R2, we used different values of the barrier height from different levels of theory in Table 3. Transition state theory (eq 6) was used to calculate the rate constant for reaction R2. Vibrational term values from Table 4 and moments of inertia from Table 5 were used. Arrhenius plots for reaction R2 from different levels of theory are shown in Figure 9, which are compared with the reported values of k_2 from the literature. The tunneling correction for reaction R2 was calculated according to eq 10 that was suggested by Shavitt[45]

$$Q_{\text{tunnel}} = 1 - \frac{1}{24}\left(\frac{h\nu^*}{k_B T}\right)^2\left(1 + \frac{k_B T}{E_0}\right)$$

where ν^* is the imaginary frequency of the activated complex at the top of the barrier, k_B and h are Boltzmann's and Planck's constants, respectively, and E_0 is the barrier height corrected for zero-point energy for the reaction. In Figure 9, Curve 1 calculated from B3LYP/6-311+G(2d,2p) results with $E_0 = 0.5$ kJ mol^{-1} by means of transition state theory, eq 6. Curve 2 is the same as curve 1 with no low vibrational term values included. Curve 3 is the same as curve 2, except $E_0 = 0.2$ kJ mol^{-1} from B3LYP/6-311++G(3df,3pd) results. Curve 4 is the same as curve 2, except no tunneling factor is included. Curve 5 is the same as curve 2, except $E_0 = 1.4$ kJ mol^{-1} from CASMP2/6-311+G(2d,2p) results. We did not show the Arrhenius plot for reaction R2 with higher barrier heights listed in Table 3. As shown in Figure 9, higher barrier heights caused a much lower rate constant from the previous reported rate constants for reaction R2. According to curve 2 in Figure 9, the rate constant of reaction R2 that corrected for tunneling factor was found as $k_2 = 9.8 \times 10^8$ L mol^{-1}s^{-1}. Curve 2 is in fair agreement with results reported in refs 11 and 12a. As discussed in the Introduction, it was difficult to deduce an accurate value for k_2 from refs 5 and 6. In ref 2, the reported value for k_2 is calculated according to the ratio of k_2/k_1. Thynne in ref 2 has calculated the value of k_2 according to a value of 1.0×10^{11} L mol^{-1}s^{-1} for k_1, which it seems is higher than the accepted values for k_1 in the literature, see Figure 5.

Conclusion

The two possible paths for the reaction of methyl radicals with ethyl radicals and dissociation of propane have been studied theoretically. All the structures and stationary points have been optimized at the MP2/6-311+G(2d,2p) level of theory. The potential energy surfaces for both reaction paths R1 and R2 were explored at a high level of quantum mechanics. To locate the bottleneck for association reaction R1, Canonical variational transition state theory, CVTST, and microcanonical variational RRKM calculations were used and the rate constant at different C- - -C distances along the reaction coordinate and at different temperatures was calculated. To use CVTST, we just considered three external rotations in each reactant, which transfer to internal, tumbling, or rocking motions as the reactants approach each other. The ratio of B_θ was found to be only a function of force constants for rocking or tumbling motions, eq 5. The bottleneck for the association rate of the two radicals or dissociation of propane at the UB3LYP surface varied from a value of 5.0 Å at lower temperatures to a value of 3.8 Å at higher temperatures. From RRKM calculations these values change from 4.90 at lower energies to 3.97 Å at higher energies. These results show it is possible to find the bottleneck for a barrier less reaction by CVTST in low cost of computation instead of using microcanonical variational RRKM calculations. According to these data, we selected the structure of transition state for reaction R1 when the reactants are 4.4 Å apart and rotational and vibrational partition functions for the transition state of reaction R1 are calculated at this point. RRKM method was used to calculate the fall off behaviors and high-pressure limiting values of k_1 and k_{-1} for association reaction R1 and dissociation reaction R−1. Calculated high-pressure limiting values of k_1 and k_{-1} are compared with the values reported in the literature in Figures 5 and 7.

For disproportionation reaction R2, the saddle point was identified at the mp2/6-311+G(2d,2p) and CAS(4,4)mp2/6-31+G(d,p) levels. The potential energy surface (IRC) was explored at the UMP2/6-311+G(2d,2p) level. According to our calculations, depending on the selected basis set, we found a barrier for reaction R2 equal to 0.2 or 0.5 kJ mol^{-1} at the UB3LYP level. At the other levels of theory, we found higher activation energies for reaction R2 (see Table 3). To the best of our knowledge, no one has reported any barrier height for reaction R2 in the literature, and almost all the reported values of k_2 are lower than the values reported for k_1 in the literature. The tunneling factor for reaction R2 was also calculated according to the Shavitt equation.[51] To the best of our knowledge, no experimental data are available for k_2 at temperatures higher than 521 K.[49] We found k_2 is independent to the temperature over the temperature range of 300−2500 K if we exclude the low vibrational term values. The reason for temperature-independent behavior of k_2 is the tunneling effect at lower temperatures.

Our results indicate that k_1 decreases as temperature increases, while k_2 is independent to the temperature. At the high pressure limit, our results show that at lower temperatures reaction R1 is more important, while at higher temperatures rates of the two reaction paths become comparable, especially if we include low vibrational term values in calculating the rate constant for reaction R2.

Acknowledgment. The authors are pleased to acknowledge financial support from the Research Council of Shiraz University.

References and Notes

(1) Grotewold, J.; Lissi, E. A.; Neumann, M. G. *J. Chem. Soc. A* **1968**, *1*, 375−381. (b) Terry, J. O.; Futrell, J. H. *Can. J. Chem*. **1967**, *45*, 2327. (c) Rotewold, J.; Lissi, E. A.; Neumann, M. G. *J. Chem. Soc. Chem. Commun*. **1966**, 1−2. (d) Grotewold, J.; Kerr, J. A. *J. Chem. Soc*. **1963**, 4337. (e) Heller, C. A. *J. Chem. Phys*. **1958**, *28*, 1255. (f) Ausloos, P.; Steacie, E. W. R. *Can. J. Chem*. **1955**, *33*, 1062.

(2) Thynne, J. C. J. *Trans. Faraday Soc*. **1962**, *58*, 676.

(3) Teng, L.; Jones, W. E. *J. Chem. Soc., Faraday Trans*. 1 **1972**, *68*, 1267.

(4) Lifshitz, A.; Frenklach, M. *J. Phys. Chem.* **1975**, *79*, 686.

(5) Koike, T.; Gardiner, W. C., Jr. *J. Phys. Chem*. **1980**, *84*, 2005.

(6) Simmie, J. M.; Gardiner, W. C., Jr.; Eubank, C. S. *J. Phys. Chem*. **1982**, *86*, 799.

(7) Anastasi, C.; Arthur, N. L. *J. Chem, Soc. Faraday Trans*. 2 **1987**, 83, 277.

(8) Garland, L. J. and Bayes, K. D. *J. Phys. Chem*. **1990**, *94*, 4941.

(9) Warnatz, J. *Combstion Chemistry*; Springer-Verlag: New York, 1984; 197.

(10) Sillesen A.; Ratajczak E.; Pagsberg P. *Chem. Phys. Let*. **1993**, *201*, 171.

(11) Tsang, W.; Hampson, R. F. *J. Phys. Chem. Ref. Data* **1986**, *15*, 1087.

(12) Baulch, D. L.; Cobos, C. J.; Cox, R. A.; Esser, C.; Frank, P.; Just, Th.; Kerr, J. A.; Pilling, M. J.; Troe, J.; Walker, R. W.; Warnatz, J. Evaluated kinetic data for combustion modeling. *J. Phys. Chem. Ref. Data* **1992**, *21*, 411−429. (b) Baulch, D. L.; Cobos, C. J.; Cox, R. A.; Esser, C.; Frank, P.; Just, Th.; Kerr, J. A.; Pilling, M. J.; Troe, J.; Walker, R. W.; Warnatz, J. Evaluated kinetic data for combusion modelling. Supplement I. *J. Phys. Chem. Ref. Data* **1994**, *23*, 847−1033.

(13) Knyazev, V. D.; Slagle, I. R. *J. Phys. Chem*. A **2001**, *105*, 6490.

(14) Warnatz, J. *Combust. Sci. Technol*. **1983**, *34*, 177.

(15) Dean, A. M. *J. Phys. Chem*. **1985**, *89*, 4600.

(16) Becker, K. H.; Kurtenbach, R. Wiesen, P. *J. Phys. Chem*. **1991**, *95*, 2390.

(17) Zhu, L.: Chen, W.; Hase, W. L. *J. Phys. Chem*. **1993**, *97*, 311.

(18) Olzmann, M. *Phys. Chem. Chem. Phys*. **2002**, *4*, 3614.

(19) Frisch, M. J.; Trucks, G. W.; Schlegel, H. B.; Scuseria, G. E.; Robb, M. A.; Cheeseman, J. R.; Zakrzewski, V. G.; Montgomery, J. A., Jr.; Stratmann, R. E.; Burant, J. C.; Dapprich, S.; Millam, J. M.; Daniels, A. D.; Kudin, K. N.; Strain, M. C.; Farkas, O.; Tomasi, J.; Barone, V.; Cossi, M.; Cammi, R.; Mennucci, B.; Pomelli, C.; Adamo, C.; Clifford, S.; Ochterski, J.; Petersson, G. A.; Ayala, P. Y.; Cui, Q.; Morokuma, K.; Malick, D. K.; Rabuck, A. D.; Raghavachari, K.; Foresman, J. B.; Cioslowski, J.; Ortiz, J. V.; Stefanov, B. B.; Liu, G.; Liashenko, A.; Piskorz, P.; Komaromi, I.; Gomperts, R.; Martin, R. L.; Fox, D. J.; Keith, T.; Al-Laham, M. A.; Peng, C. Y.; Nanayakkara, A.; Gonzalez, C.; Challacombe, M.; Gill, P. M. W.; Johnson, B. G.; Chen, W.; Wong, M. W.; Andres, J. L.; Head-Gordon, M.; Replogle, E. S.; Pople, J. A. *Gaussian 98*, revision A.3; Gaussian, Inc.: Pittsburgh, PA, 1998.

(20) Krishnan, R.; Pople, J. A. *Int. J. Quantum Chem*. **1978**, *14*, 91. Krishnan, R.; Frisch, M. J.; Pople, J. A. *J. Chem. Phys*. **1980**, *72*, 4244.

(21) Roos, B. O. *Adv. Chem. Phys*. **1987**, *69*, 399.

(22) Becke, A. D. *J. Chem. Phys*. **1993**, *98*, 5648.

(23) Pople, J. A.; Head-Gordon, M.; Raghavachari K. *J. Chem. Phys*. **1987**, *87*, 5968. Cizek, J. *Adv. Chem. Phys*. **1969**, *14*, 35. Scuseria, G. E. Schaefer, H. F. III *J. Chem. Phys*. **1989**, *90*, 3700.

(24) Curtiss, L. A.; Raghavachari K.; Trucks, G. W., and Pople, J. A. *J. Chem. Phys*. **1991**, *94*, 7221.

(25) Gurvich, L. V.; Veyts, I. V.; Alcock, C. B. *Thermodynamic Properties of Individual Substances*, 4th ed.; Hemisphere Pub. Co.: New York, 1989.

(26) Frenkel, M.; Marsh, K. N.; Wilhoit, R. C.; Kabo, G. J.; Roganov, G. N. *Thermodynamics of Organic Compounds in the Gas State*, Thermodynamics Research Center: College Station, TX, 1994.

(27) Pacey, P. D. *J. Phys. Chem. A* **1998**, *102*, 8541.

(28) P. D. Pacey, *J. Chem. Phys*. **1982**, *77*, 3540.

(29) Mousavipour, S. H.; Emad L.; and Fakhraee S. *J. Phys. Chem*. **2002**, *106*, 2489.

(30) Quack, M.; Troe, *J. Ber. Bunsen-Gas. Phys. Chem*. **1974**, *78*, 240. Wardlaw, D. M.; Marcus, R. A. *Chem. Phys. Lett*. **1984**, *110*, 230. *J. Chem. Phys*. **1985**, *83*, 3462. Robertson, S. H.; Wagner, A. F.; Wardlaw, D. M. *J. Chem. Phys*. **1995**, *103*, 2917.

(31) Benson, S. W. *Thermochemical Kinetics*, 2nd ed.; Wiley: New York. 1976.

(32) Hase, W. L.; Zhu, L. *Int. J. Chem. Kinetics*, **1994**, *26*, 407. Smith, S. C. *J. Phys. Chem*. **1993**, *97*, 7034. Hase, W. L. *Acc. Chem. Res*. **1983**, *16*, 258.

(33) Zhu, L.; Hase, W. L. *QCPE Program 644*; Quantum Chemistry Program Exchange, Indiana University: Bloomington, IN.

(34) Truhlar, D. G.; Isaacson, A. D.; Garrett, B. C. *Theory of Chemical Reaction Dynamics*; Baer, M., Ed.; CRC Press: Boca Raton, FL, 1985.

(35) Wigner, E. P. Z. *Phys. Chem.* B **1932**, *19*, 203.
(36) Holbrook, K. A.; Pilling, M. J.; and Robertson, S. H. *Unimolecular Reactions*, 2nd ed.; John Wiley & Sons Ltd.: Chichester, England, 1996.
(37) Wardlaw, D. M.; Marcus, R. A. *J. Phys. Chem*. **1986**, *90*, 5383.
(38) Tardy, D. C.; Rabinovitch, B. S.; Whitten, G. Z. *J. Chem. Phys*. **1968**, *48*, 1427.
(39) Zhu, L.; Chen, W.; Hase, W. L. *J. Phys. Chem.* **1993**, *97*, 311.
(40) *Handbook of Chemistry and Physics*, 80th ed.; Lide, D. R., Ed.; CRC Press: Boca Raton, FL, 1999−2000.
(41) Jacox, M. E. *J. Phys. Chem. Ref. Data*, Monograph 3, **1994**.
(42) Shimanouchi, T. *Tables of Molecular Vibrational Frequencies*; NSRDS−NBS-39; American Chemical Society and the American Institute of Physics for the National Bureau of Standards: New York, 1972, Consolidated Vol. 1.
(43) *NIST Chem. Kinetics Database*, Ver. 2Q98. 1998.
(44) Belmeliani, A.; Perrin, D.; Martin, R. *J. Chim. Phys*. **1994**, *91*, 313. (b) Tsang, W. *Combust. Flame* **1989**, *78*, 71. (c) Hidaka, Y.; Oki, T.; Kawano, H. *Int. J. Chem. Kinet*. **1989**, *21*, 689. (d) Dombi, A.; Horvath, I.; Huhn, P. *Int. J. Chem. Kinet*. **1986**, *18*, 255. (e) Warnatz, J. *Combustion Chemistry*, W. C. Gardiner, Jr., ed.; Springer-Verlag: NY, 1984; p 197.
(45) Shavitt, I. *J. Chem. Phys*. **1959**, *31*, 1359.
(46) Tsang, W. *Combust. Flame* **1989**, *78*, 71.
(47) Laufer, A. H.; Gardner, E. P.; Kwok, T. L.; Yung, Y. L. *Icarus*, **1983**, *56*, 560.
(48) Kanan, K.; Purnell, H.; Smith, E. *Int. J. Chem. Kinet.* **1983**, *15*, 63.
(49) Arthur, N. L.; Anastasi, C. *Bull. Soc. Chim. Belg.* **1983**, *92*, 647.
(50) Halstead, M. P.; Leathard, D. A.; Marshall, R. M.; Purnell, J. H. *Proc. R. Soc. Londen A* **1970**, *316*, 575.
(51) Heller, C. A. *J. Chem. Phys*. **1958**, *28*, 1255.